

**České vysoké učení technické v Praze
Fakulta stavební**

**Czech Technical University in Prague
Faculty of Civil Engineering**

doc. RNDr. Igor Medved', PhD.

**Teoretické aspekty transportu tepla, vlhkosti a solí v porézních
stavebních materiálech**

**Theoretical aspects of heat, moisture, and salts transport in porous
building materials**

Summary

In this lecture I give a brief overview of selected theoretical aspects of heat, moisture, and salts transport in porous building materials on which I have been working in the Department of Materials Engineering and Chemistry since 2010. The work was supported significantly by two grants: Cumulative time dependent processes in building materials and constructions (Czech Science Foundation grant No. P105/12/G059) and Complex system of methods for controlled design and assessment of functional properties of building materials (Ministry of Education grant No. MSM: 6840770031).

The initial impulse for my research was a striking controversy: the diffusion coefficient of salts transported through a lime-based plaster, sandstone, and similar materials turned out to be way too high in comparison with its value for pure water. The challenge was to suggest suitable experiments to identify the additional effects causing this behavior and to propose appropriate transport models to analyze them.

Two such additional effects could provide the explanation. One is surface diffusion (see Section 3) and the other is osmosis (see Section 4). Either has not been studied for building materials in much depth yet. I suggested to apply one experimental method to analyze each of them: the time-lag method and the Sherwood–Cruster method, respectively. My colleagues have been already testing and using the former one, but the results still do not seem to be quite reliable; the latter method is yet to be performed. I also worked on a microscopic description of surface diffusion, using my previous experience from statistical mechanics of lattice gases. We were able to obtain a simple formula for the surface diffusion coefficient when a first-order phase transition occurred on the surface (see Section 3). In addition to these efforts, I suggested to derive formulas for a fast calculation of varying diffusion coefficients by the Boltzmann–Matano method (see Section 5), which is usually done numerically and may be pretty time consuming. We were successful and were even able to compare the results when various theoretical profiles were used to approximate a given experimental profile.

Souhrn

V této přednášce uvádím stručný přehled vybraných teoretických aspektů přenosu tepla, vlhkosti a solí v porézních stavebních materiálech, na kterých jsem pracoval na Katedře materiálového inženýrství a chemie od roku 2010. Tato práce byla výrazně podpořena dvěma granty: Kumulativní časově závislé procesy ve stavebních materiálech a konstrukcích (projekt GAČR č. P105/12/G059) a Komplexní systém metod pro řízený návrh a hodnocení funkčních vlastností stavebních materiálů (projekt MŠMT č. MSM: 6840770031).

Původním impulsem pro můj výzkum byl tento zarážející rozpor: difúzní koeficient solí přenášených ve vápenné omítce, pískovci a podobných materiálech se ukázal být mnohem vyšší v porovnání s jeho hodnotou pro čistou vodu. Výzvou bylo doporučit vhodné experimenty na identifikování dodatečných efektů způsobujících toto chování a navrhnout příhodné transportní modely na jejich analýzu.

Dva takové dodatečné efekty by mohly poskytnout vysvětlení. Jedním je povrchová difúze (viz Sekce 3) a druhým je osmóza (viz Sekce 4). Ani jeden z nich nebyl doposud v případě stavebních materiálů podrobněji studován. Doporučil jsem aplikovat jednu experimentální metodu na analýzu každého z nich: metodu opožděného času, resp. Sherwood–Crusterovu metodu. Moji kolegové již testují a používají první metodu, ale výsledky se zatím nezdaří být celkem spolehlivé; druhá metoda ještě musí být provedena. Pracoval jsem také na mikroskopickém popisu povrchové difúze, přičemž jsem použil své dřívější zkušenosti ze statistické mechaniky mřížkových plynů. Byli jsme schopni získat vzorec pro povrchový difúzní koeficient, když na povrchu dochází k fázovému přechodu prvního druhu (viz Sekce 3). Kromě těchto snah jsem navrhnul odvodit vzorce umožňující rychlý výpočet měnících se difúzních koeficientů pomocí Boltzmann–Matanovy metody (viz Sekce 5), který se obvykle provádí numericky a je časově dost náročný. Byli jsme úspěšní, a dokázali jsme dokonce porovnat výsledky, když se použijí různé teoretické profily na aproximování daného experimentálního profilu.

Klíčová slova

porézní těleso, transportní model, difúzní koeficient, koncentrace solí, povrchová difúze, osmóza, inverzní metody

Kyewords

porous body, transport model, diffusion coefficient, salt concentration, surface diffusion, osmosis, inverse methods

Contents

1	Introduction	6
2	Modeling of transport in porous materials	8
3	Surface diffusion	11
3.1	Experimental investigation	12
3.2	Theoretical investigation	16
4	Osmosis	19
5	Boltzmann–Matano method	23
	Bibliography	28
	Curriculum Vitae	32

1 Introduction

Proper understanding of heat, moisture, and salt transport in porous building materials is crucial for the assessment of their performance and durability. In fact, moisture and salt can cause serious deterioration and structural damages to these materials, for example, due to the corrosion of steel in concrete structures and salt efflorescence. Heat may significantly affect the materials dimensions and cause length changes responsible for cracks in concrete structures. Instead of employing destructive methods that ruin samples, it is convenient to describe the transport by suitable models. This approach has also the potential to predict future behavior in the long run, which may require years of investigations if only experimental methods are applied.

The accuracy of modeling critically depends on several factors. First, it is the model itself in which heat, water, and salt transport should be coupled (salts can be transported only in the presence of water, and isothermal conditions are rare in practice). Second, it is the initial and boundary conditions that are specified from an experimental on-site analysis or suitably adjusted in a laboratory measurement. Finally, it is the precision with which one can determine the input transport and storage parameters that appear in the model, because they may strongly depend on the water content, salt concentration, or temperature. In that case the traditional methods of their determination (from fitting the model with constant parameters to measured profiles) cannot be applied. Rather, the parameters are often determined by inverse methods.

Microscopic modeling is another approach that may significantly contribute to the understanding of mass and heat transport. This is usually a very complex task, and often very simple models can be only investigated (so that the corresponding results need not be actually useful in real applications). Nevertheless, this approach may bring completely new insight into some problems and, with the help of powerful computer techniques (for example, molecular dynamics simulations and density-functional calculations), even produce interesting practical results.

In this lecture I shall present my recent results in the transport of moisture, salts, and heat in porous building materials based on both macroscopic and microscopic models.

2 Modeling of transport in porous materials

There are various types of models used to describe mass and heat transport in porous materials. A natural way to model the transport of water is to use *convection* as the dominant mechanism. For an unsaturated case the water flux $\mathbf{J} = \rho \mathbf{v}$ (where ρ is the water density and \mathbf{v} is the Darcy velocity) satisfies the continuity equation for the water mass balance in a porous body. Neglecting the gravity effects and assuming that water is incompressible, this equation may be written as [1]

$$\frac{\partial w}{\partial t} = \nabla \cdot [\kappa(w) \nabla w]. \quad (2.1)$$

Here the moisture diffusivity κ describes the liquid water transport and the volumetric moisture content w is the driving force. This formulation is appropriate in building physics, and it is equivalent to the formulation via the water permeability or hydraulic conductivity frequently employed in soil science, where the driving force is associated with the capillary water pressure and hydraulic head, respectively [2, 3].

For the transport where water vapor is included *diffusion* is mostly the dominant mechanism. In this case the simplest model is the standard diffusion equation, analogous to Eq. (2.1), with the driving force being the moisture content by mass, u , and the moisture transport described by the diffusion coefficient, $D(u)$ [1]. Both u and D are sums of water vapor and liquid water contributions.

In *hybrid* models both diffusion and convection are combined. A simple example of this sort can be obtained from the linear theory of mixtures. Applying the mass balance equation for moisture in which the total flux is the sum of a diffusion term, $-\kappa_d(u) \nabla \rho$, and convection term, $\rho \mathbf{v}$, the model may be written as [1]

$$\frac{\partial u}{\partial t} = (1 + u) \nabla \cdot [\kappa_d(u) \nabla u] + \kappa_d(u) (\nabla u)^2, \quad (2.2)$$

provided the solid matrix is nondeformable and of constant density.

A systematic approach to formulate models of transport, especially when the situation is more complex and heat and/or salts are transferred besides moisture, is to apply the rules of non-equilibrium thermodynamics [4]. These imply that a correct identification of the thermodynamic forces, \mathbf{X}_i , and fluxes, \mathbf{J}_i , in a model of a specific transport problem requires to rewrite the entropy production rate as a sum of terms of the form $\mathbf{J}_i \cdot \mathbf{X}_i$. To do so, one usually combines the balance equations with thermodynamic laws. Moreover, the rules imply the presence of various *cross effects*, such as the Soret and Dufour phenomena.

A simple example is a model of a diffusive heat and liquid moisture transport in a porous body under isobaric conditions when phase changes are neglected. This model may be formulated as [1]

$$\frac{\partial c}{\partial t} = \nabla \cdot (D \nabla c + \delta \nabla T), \quad (2.3)$$

$$\rho_t c_p \frac{\partial T}{\partial t} = \nabla \cdot (k_c \nabla c + \lambda^* \nabla T), \quad (2.4)$$

where $c = (\rho/\rho_t)w$ is the moisture mass concentration, T is the thermodynamic temperature, ρ_t is the body's density, and c_p is the isobaric specific heat capacity. Note that the transfer of heat and moisture are *coupled* in this model: time changes in the concentration and temperature are induced by spacial changes in both of them. The direct (c - c and T - T) effects are described by the diffusion coefficient D and a generalized thermal conductivity λ^* , while the cross (c - T and T - c) effects by the Soret and Dufour coefficients δ and k_c .

When the transport of salts (or chemical compounds in general) occurs, diffusion models are usually employed. They are based on Fick's law according to which the mass flux of a salt is proportional to the gradient of the salt mass concentration, $\mathbf{J}_s^{\text{diff}} = -D_s \nabla c_s$, where D_s is the salt diffusion coefficient. This simple picture may require several improvements. One is the fact that salts can move through a porous body only in the presence of water. Thus, besides the diffusive part, the total salt flux must contain a convective part, $\mathbf{J}_s^{\text{conv}} = \rho_t c_s \mathbf{v}_{\text{drift}}$, leading to the coupling of water and salt transports. Another improvement is needed when the salt species are not electrically neutral. Then electrical interactions must be considered, adding a part $\mathbf{J}_s^{\text{el}} \propto \nabla \varphi$ to the total flux that is proportional to the gradient of an electric potential (expressed mostly by the Nernst-Planck equation). An improvement due to possible chemical reactions that cause the production of salts may be also needed. This is implemented via a suitable source term in the balance equations. As a result, rather complex models of coupled

water, salts, and heat transport through porous bodies may arise.

To illustrate the point, let us mention the sophisticated model of Koniorczyk and Gawin [5] that consists of as many as *five* balance equations. One is for the mass balance of liquid water and vapor, one for the mass balance of a salt dissolved in the fluid phase, one for the mass balance of dry air, one for the enthalpy of the porous body, and one for its linear momentum. Using computer simulations, this model has been quite successfully applied to the investigation of practical problems related to the moisture and heat transport in building materials containing salt. These included capillary suction by sandstone, osmosis in cement mortar, influence of salt on drying of a building element [5], or salt crystallization in a brick wall [6].

Of course, when trying to understand a specific problem, it is desirable to employ a model that is as simple as possible but, at the same time, plausible to capture the main aspects of the problem. Still, even simple models may require the use of computer simulations to be solved. However, good care must be taken not to oversimplify the situation, because the ‘standard’ simple models that are widely used can lead to *controversial results*. An example may be a coupled water and chloride transport in a lime plaster studied in [7, 8]. For water saturated samples the values of the chloride diffusion coefficient were found to be very close to the value of the coefficient in pure water (of order $10^{-9} \text{ m}^2\text{s}^{-1}$). It is therefore possible to conclude that a simple diffusion mechanism was dominant for the chloride transport. On the other hand, for the penetration of chloride solution into dry samples, the diffusion coefficient was found to be about three orders of magnitude higher than for water saturated samples. This sudden acceleration of the chloride transport suggest that *additional effects* must be present, such as surface diffusion and osmosis [7, 8]. It is primarily the study of these effects that I shall discuss in this lecture.

3 Surface diffusion

Besides the usual bulk diffusion in pores, particles can migrate across a porous material along the pores surface. Bulk diffusion is driven by a concentration gradient of the migrating particles, and there is no interaction between the particles and the inner walls of the pores (except, perhaps, collisions). However, particles may adsorb on these walls and diffuse on the surface while being adsorbed (i.e., while being within the potential field of adsorption). This particle migration is called surface diffusion (see Fig. 3.1) and can be experimentally observed and probed by nuclear magnetic resonance methods [9, 10]. It can *significantly contribute* to the total mass transfer rate in porous materials both in gas-solid and liquid-solid adsorption systems. For example, in reversed-phase liquid chromatography systems, the bulk diffusivity is about one order less than the total diffusivity, so that more than 90 % of the particles migrate by surface diffusion [11, 12].

Surface diffusion is complicated by a complex nature of the interactions between the adsorbate particles and the surface atoms as well as by the complexity of the surface. The lateral interactions—those between the diffusing particles themselves—must be also taken into account. As usual, there are two approaches to study surface diffusion: experimental and theoretical. Let us briefly discuss both.

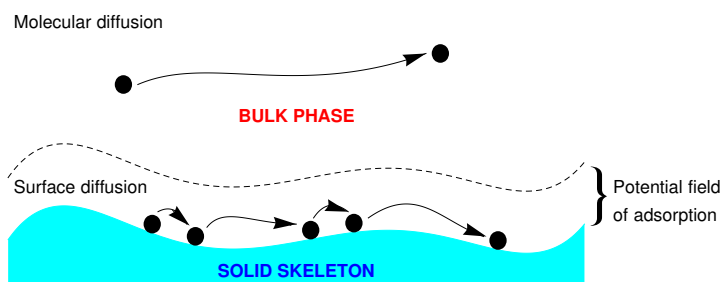


Figure 3.1: An illustration of surface and molecular diffusions.

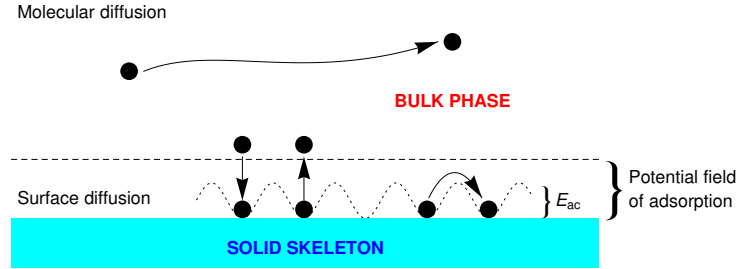


Figure 3.2: An illustration of surface diffusion as an activated process. The periodic energy barrier is depicted by a dotted line, and the activation energy E_{ac} is indicated.

3.1 Experimental investigation

In the experimental approach the surface diffusion coefficient, D_s , is obtained from measurements as a function of the involved parameters (the surface concentration and temperature) for a given solid material. Clearly, such results are limited to the given system and may not be extensible to other systems. Still, some kinetic theory must be proposed to explain these results. Various theories of this sort have been proposed, and they may be split into three categories [13,14].

First, theories based on hopping models in which the migrating particles are viewed as hopping between distinct, energetically favorable adsorption sites on the surface. Thus, surface diffusion is viewed as an activated type of a mass transfer process: if an adsorbed particle acquires a sufficient energy, called the activation energy, E_{ac} , it can get over the energy barrier between adsorption sites and jump to a neighboring site (see Fig. 3.2). Hopping models are appropriate when at most one layer of adsorbed particles is formed.

Second, theories based on hydrodynamic models in which the diffusion of adsorbed particles is due to the viscous motion of the liquid film inside the porous medium. These models are not used very often because a hydrodynamic flow appears only when at least a few layers of adsorbed particles are formed.

Third, theories based on Fickian models in which surface diffusion is treated as the flow in excess of bulk diffusion. If the two flows are independent, the total flux becomes the sum

$$\mathbf{J}_t = \mathbf{J}_b + \mathbf{J}_s, \quad (3.1)$$

and the surface diffusion flux \mathbf{J}_s is obtained as the total diffusion flux minus

the diffusion flux of a non-adsorbing fluid. This method underestimates the bulk flux and overestimates the surface flux because the path ‘desorption \rightarrow bulk diffusion \rightarrow re-adsorption’ is neglected.

At present it is sometimes difficult to place a given kinetic model in only one of the above three categories, because it may take into account two or more dominant mechanisms of surface diffusion.

The basic experimental approach to evaluate the surface diffusivity is to measure a physical quantity that is sufficiently sensitive to the surface diffusivity. Then the latter along with its dependence on the temperature and/or concentration follow when the model is tested against experimental data.

From the practical point of view, the surface diffusion flux is related to the gradient of the surface concentration by the Fickian equation

$$\mathbf{J}_s = -D_s \nabla c_s, \quad (3.2)$$

where c_s is the surface concentration of the transported particles. The surface diffusivity D_s may strongly depend on c_s and T as well as on the interaction between the adsorbate and the solid surface and the structure of the solid surface. Even though Eq. (3.2) often correctly describes the surface diffusion flux, the fundamental question is the exact functional form of D_s . In fact, it is the dependence of D_s on many parameters that makes the study of surface diffusion very complicated.

In [15] we compared four experimental methods from which the surface diffusivity can be obtained from an appropriate analysis of measured data. We concluded that the *time-lag method* is most convenient of them, because its kinetic model is easy to solve numerically and the separation of D_s from the bulk diffusivity, D_b , is more reliable. In this method a sample is situated between two chambers, one of which (the upstream chamber) is filled with an adsorbate particles and the other (the downstream chamber) is initially isolated from the sample and is empty. The upstream chamber is, at an initial time, opened and the diffusion of adsorbate particles through the sample begins. For some time, the amount, Q , permeating out of the sample to the downstream chamber is negligible because the particles are accumulated in the sample. However, after most of the adsorbed sites inside the sample are equilibrated, Q starts rising until it reaches a linear asymptote, $Q(t) \approx S_\infty(t - t_{\text{lag}})$ (see Figs. 3.3 and 3.4). In a Q vs. t plot, the asymptote intersects the time axis at a time, t_{lag} , called the lag time, that represents the time required for the particles to spend its life within the sample. The time lag is a function of the operating conditions and kinetic

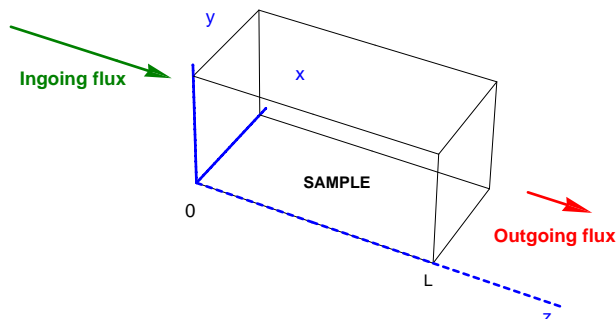


Figure 3.3: A scheme of an experimental set-up for the time-lag method.

parameters, including the bulk and surface diffusivities. Thus, obtaining time lag experimentally allows one to determine these diffusivities.

The kinetic model corresponding to the time-lag method is based on the following assumptions. First, the system is isothermal ($T = \text{const}$). This is not a serious restriction and can be easily achieved experimentally. Second, the adsorbed particles are in a local equilibrium with bulk particles in pores so that an adsorption isotherm equation, $c_s = g(c_b)$, is applicable. It is then necessary to measure the adsorption isotherm for a given material and use a suitable isotherm equation that fits the data (such as the Langmuir or BET equation) or a numerical approximation of the data. Third, the mass transport is given by the bulk diffusion flux, \mathbf{J}_b , and surface diffusion flux, \mathbf{J}_s , that are in the direction of the sample coordinate z (see Figs. 3.3 and 3.4). In experiment this is arranged by isolating the four faces of the sample parallel with the z direction. If c_b is not high (no capillary condensate flow occurs), then the total mass concentration and total mass flux are

$$c_t = \varepsilon c_b + (1 - \varepsilon)c_s, \quad \mathbf{J}_t = \varepsilon \mathbf{J}_b + (1 - \varepsilon)\mathbf{J}_s, \quad (3.3)$$

where

$$\mathbf{J}_b = -D_b \nabla c_b, \quad \mathbf{J}_s = -D_s \nabla c_s, \quad (3.4)$$

and $0 < \varepsilon < 1$ is the fraction of the pore volume in which transported particles are beyond the influence of the adsorption field. Finally, D_b and ε are constants, c_b and c_s depend only on z and time t , and $D_s(c_s)$ satisfies the Darken expression $D_s = D_{s0}(\partial \ln c_b / \partial \ln c_s) = D_{s0}(c_s / g'(c_b) c_b)$ (here D_{s0} is the surface diffusivity at zero loading).

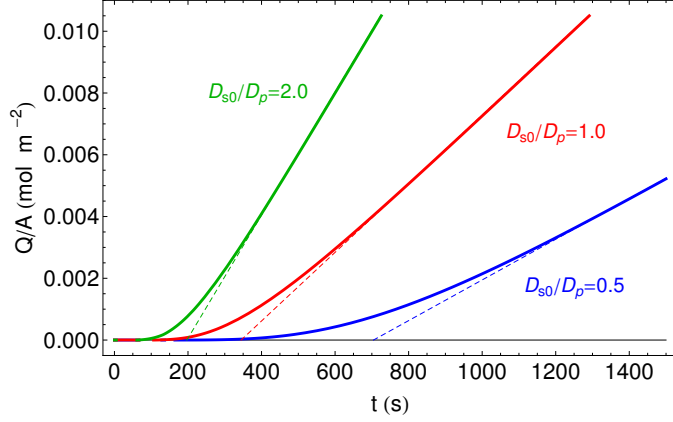


Figure 3.4: The plots the permeating amount vs. time obtained from a numerical solution of the model, Eq. (3.5) (adapted from Fig. 7(a) in [15]). The sensitivity of the curves to a change in D_{s0} is illustrated by using three values of D_{s0} . The corresponding values of t_{lag} are found at the intersections of the linear asymptotes with the horizontal axis (indicated by dashed lines).

The resulting time-lag model follows from the overall mass balance equation and may be written as

$$G(c_b(z, t)) \frac{\partial c_b(z, t)}{\partial t} = \frac{\partial}{\partial z} \left[H(c_b(z, t)) \frac{\partial c_b(z, t)}{\partial z} \right] \quad (3.5)$$

with

$$G(c_b) \equiv \varepsilon + (1 - \varepsilon)g'(c_b), \quad H(c_b) \equiv \varepsilon D_b + (1 - \varepsilon)D_{s0} \frac{g(c_b)}{c_b}, \quad (3.6)$$

where the prime indicates the derivative. Measuring or estimating ε and D_b independently, the only fitting parameter is D_{s0} . The initial condition reads $c_b(z, 0) = 0$ (the sample contains no adsorption particles at the beginning). One boundary condition is $c_b(0, t) = c_0$ (a constant supply of adsorbent from the inlet side of the sample) and the other one may be chosen as the Dirichlet condition $\partial c_b(L, t)/\partial z = \text{const}$ (the constant is to be taken from experimental data). It is not necessary to solve the mass balance equation (3.5) to obtain the time lag. Indeed, the approach of Frisch [16] applied to the model yields the formula [17]

$$t_{\text{lag}} = L^2 \frac{\int_{c_L}^{c_0} H(\xi) \left(\int_{\xi}^{c_0} H(c) dc \right) \left(\int_0^{\xi} G(c) dc \right) d\xi}{\left(\int_{c_L}^{c_0} H(c) dc \right)^3}, \quad (3.7)$$

where c_0 and c_L are the steady-state concentrations at $z = 0$ and $z = L$, respectively. As soon as the isotherm equation is known, the time lag may be readily evaluated from this formula, yielding an explicit relationship of the time lag to the surface diffusivity. Therefore, experimental data on t_{lag} provide a straightforward way of obtaining D_s .

3.2 Theoretical investigation

The theoretical approach requires the ‘complete’ knowledge of the surface structure and a detailed understanding of the interactions between the surface atoms and the diffusing particles as well as the interactions between the diffusing particles themselves (lateral interactions). Given such knowledge, approximate dynamical methods (often Monte Carlo and molecular dynamics simulations) are used to study the mobility of particles in the close neighborhood of the surface atoms [18, 19]. Although this approach is more fundamental and can be used as a predictive tool, the complete knowledge of real surfaces is usually not available. In addition, solving the problem even by the approximate methods is often a very complex task.

A very popular way to simulate surface diffusion is to employ *lattice-gas models*. In these models the migration of adparticles is given by the potential relief of the substrate surface: most of the time the adparticles stay at fixed positions (sites) where the relief attains its minima, but from time to time they perform random jumps to the adjacent vacant sites (see Fig. 3.2 and 3.5). Assuming the jumps to be instant, the states of the system of adparticles are represented by occupation numbers (one number for each site), like in a lattice gas. Although this description is rather oversimplifying, it should possess the key aspects of the diffusion and, moreover, it can be treated by a number of statistical mechanical methods, such as the mean-field, real-space renormalization group, and computer simulation techniques [18].

We contributed to this line of investigation by determining rigorous expression for the surface diffusivity D_c , using the Borgs–Kotecký theory of first-order phase transitions [20]. Near such a transition, where two phases coexist, the surface concentration (coverage) exhibits a sharp jump between two values, θ_1 and θ_2 . We showed [21] that the diffusion coefficient behave as the sum of two hyperbolas,

$$D_c \approx \frac{A_1}{N|\theta - \theta_1|} + \frac{A_2}{N|\theta - \theta_2|}, \quad (3.8)$$

where N is the number of adparticles in the system. This behavior rapidly

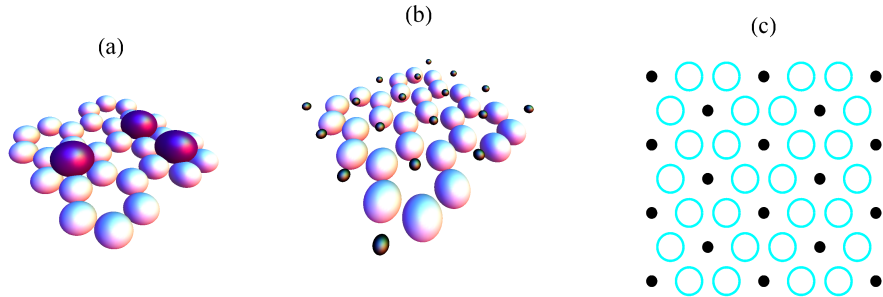


Figure 3.5: (a) Particles of an idealized hexagonal metallic surface with three particles adsorbed onto the surface. (b) The surface with the adsorption positions indicated (black spheres). (c) Two-dimensional representation of the adsorption positions forms a triangular lattice (surface particles are indicated by circles).

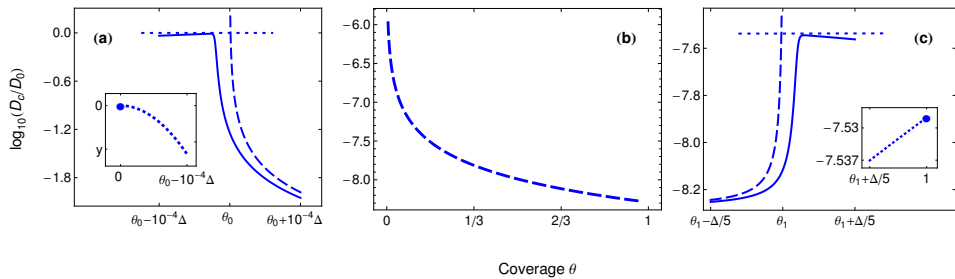


Figure 3.6: The coverage dependence of the logarithm of the surface diffusion coefficient (relative to the diffusion coefficient of noninteracting particles D_0) in the region of (a) the fully vacant phase, (b) phase coexistence, (c) the fully occupied phase for $N = 30 \times 40$, $\varepsilon_b = -5\varepsilon_t/3$, and $\varepsilon_t = 4k_B T$. The dashed lines correspond to the two-phase region (Eq. (3.8)), dotted lines to single-phase regions, and the full lines to crossover regions. The values $\Delta = N^{-3/4}$ and $y = -1.2 \times 10^{-11}$.

changes as the system goes to either of the single-phase regimes. The crossover behavior (between the two-phase and single-phase regimes) is described by rather complex formulas.

As an example, we considered a model in which particles could be adsorbed on a solid surface only at sites forming a regular triangular lattice. Each lattice site was either vacant or occupied. The lateral interactions were assumed to be between a pair of nearest-neighbor adparticles (with an energy ε_b) and a triple of nearest-neighbor adparticles (with an energy ε_t). The model can have four possible phases: fully vacant, fully occupied, and two phases with a partial occupancy $1/3$ and $2/3$ (in which one sublattice of the triangular lattice is occupied/vacant). For the transition between the

fully vacant and fully occupied phase with ε_t repulsive and ε_b attractive the dependence of D_c on the coverage is plotted in Fig. 3.6. Our other works on this topic was published in [22–25].

4 Osmosis

A porous material may act as a semipermeable membrane that allows the migration of a solvent (usually water) and restricts the passage of solute molecules (salts) or ions (see Fig. 4.1). This transport of water, when a fluid flows from the region with a low solute concentration (a high fluid chemical potential) to the region with its high concentration (a low fluid chemical potential), is called osmosis [26]. The flow increases the fluid pressure in the latter region (see Fig. 4.2) and decreases it in the former one. These pressure changes lead to a countering hydraulic flow, until the two opposing flows cancel each other and equilibrium is reached. The development of overpressures and high salinities due to osmotic effects may be of significant concern in many applications. In fact, in the past decade or so the transport of species through porous media by coupled effects, and by osmosis in particular, has attracted much attention in geophysics, environmental sciences, civil engineering, or petroleum industry.

Osmosis can be caused not only by a concentration gradient (chemical osmosis) but also by gradients in the electric potential (electro-osmosis) or temperature (thermo-osmosis). In fact, an electric potential difference can force a fluid to flow into or out of the material. In addition, under a temperature gradient, a fluid may flow from hot to cold region or vice versa, depending on the entropy difference between the fluid inside the material and

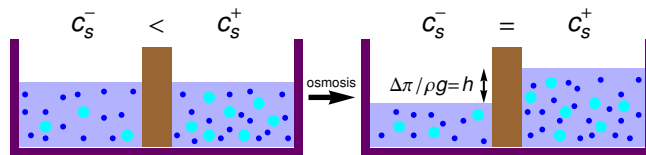


Figure 4.1: A schematic representation of chemical osmosis. A porous material (in the center) that can act as a semipermeable membrane permits the passage of the solvent (the small disks) but not of the solute (the large disks). The hydrostatic pressure increases in the compartment of higher solute concentration until the osmotic pressure $\Delta\pi = \rho gh$ is reached and the solvent concentrations in both compartments equalize.

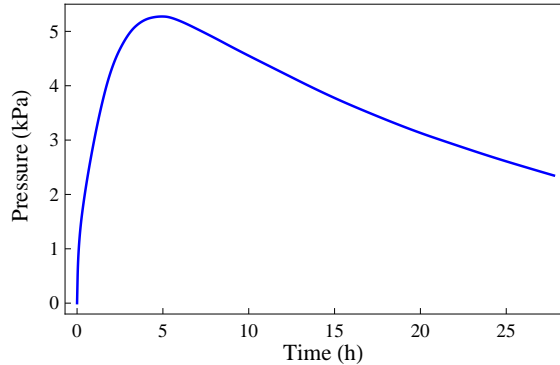


Figure 4.2: A typical time evolution of the fluid pressure in a chemical osmosis experiment in a high concentration region (adapted from [9]). The initial increase is caused by the osmotic flow into the region, while the final decline by diffusion out of the region. The maximal pressure value is equal to $\sigma\Delta\pi$.

outside it. For example, water in a hydrophilic material can be considered to have a relatively ordered state compared to water existing outside the material, leading to a water flow from the cold side to the hot one. On the other hand, for hydrophobic materials water usually flows in the opposite direction. In addition, the membrane behavior is sometimes due to pore dimensions (steric hindrance, i.e., if the solute molecule is greater than the pore size) or, say, electric fields that block ions from entering the pores, while water and non-charged solutes are freely admitted to the material.

The studies of osmosis mostly focus on the behavior of clays or similar materials, but porous building materials have been only rarely investigated. This is rather surprising because their microscopic properties may be very similar to clays and osmotic phenomena should be expected to play a significant role in the transport of solutes through them. If these are not taken into account, serious inaccuracies may arise in modeling and interpretation of the transport. On the other hand, the membrane behavior need not be relevant in all applications. Therefore, each application must be given its own consideration.

The ability of a material to act as an osmotic membrane is quantitatively characterized by the *osmotic efficiency* (also called the reflection coefficient), σ . Its value ranges between two extremes: 0 for a non-permselective material and 1 for a material with the perfect or ideal membrane behavior. It is not rare that σ can attain rather high values, about 0.75, or be even close to 1. Direct experimental evidence for osmosis was provided for materials like clays and zeolite-clays, cement mortar, or silica-zirconia [26].

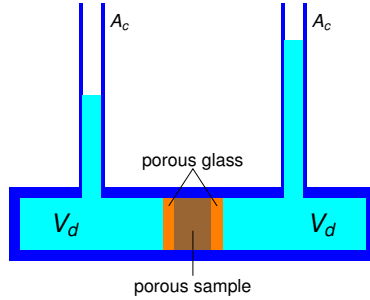


Figure 4.3: A scheme of the apparatus used by Sherwood and Craster. Both the reservoirs have the same volume, V_d , and the capillaries cross sections A_c .

Sherwood and Craster [27] proposed a low-pressure device from which the Darcy permeability κ , salt diffusivity D_s , and osmotic efficiency σ can be determined. Namely, a sample is placed between two reservoirs with the same salt solutions of different initial concentrations (see Fig. 4.3). A capillary of the cross-sectional area A_c is inserted into either reservoir to detect volume changes of the fluid. The differences Δp and Δx_s in the pressure and salt mole fraction between the two reservoirs (i.e., across the membrane) are monitored as functions of time. Using a theoretical model that considers only the hydraulic and chemical-osmosis effects, the dependences may be written in terms of decaying exponentials

$$\Delta p(t) = a_1(e^{-a_2 t} - e^{-a_3 t}), \quad \Delta x_s(t) = \Delta x_s^0 e^{-a_3 t}, \quad (4.1)$$

where a_i are specific functions of κ , D_s , and σ , and Δx_s^0 is the salt mole fraction at an initial time. Upon fitting experimental data on $\Delta p(t)$ and $\Delta x_s(t)$ with these theoretical functions, one can determine κ , D_s , and σ .

A simple example of a macroscopic model of chemical osmosis based on non-equilibrium thermodynamics that was used to predict the evolution of pressure and salinity in a clay membrane was proposed by Bader and Kooi [28]. The mass balance equations were the sourceless continuity equations for isothermal liquid and solute transport in a porous medium,

$$\frac{\partial(n\rho_f)}{\partial t} + \nabla \cdot (\rho_f \mathbf{J}_t) = 0, \quad \frac{\partial(nc_s)}{\partial t} + \nabla \cdot \mathbf{J}_s = 0, \quad (4.2)$$

where n is the porosity and ρ_f is the fluid (solution) density. The total (solution) and salt mass fluxes are given as

$$\mathbf{J}_t = -\frac{\kappa}{\mu} \left[\nabla p - \sigma \nu R T \rho_f \nabla \left(\frac{c_s}{\rho_f} \right) \right], \quad \mathbf{J}_s = (1 - \sigma) c_s \mathbf{J}_t - D_s (1 - \sigma) \nabla c_s, \quad (4.3)$$

where μ ($\text{kg m}^{-1}\text{s}^{-1}$) is the dynamic viscosity of the fluid and ν is the dissociation coefficient. Note that for $\sigma = 0$ the two flux expressions in Eq. (4.3) reduce to Darcy's law and to Fick's law for solute transport by advection and diffusion, respectively. On the other hand, for $\sigma = 1$ there is no solute transport, while solution transport may be significant due to both hydraulic and osmotic gradients. The pressure evolution for this model calculated numerically for a 1D flow through a 1-cm thick membrane with $\sigma = 0.1$, $k = 10^{-8} \text{ m}^2$, $D = 10^{-9} \text{ m}^2\text{s}^{-1}$, and $n = 0.3$ is shown in Fig. 4.2.

It should be noted that further insight into osmotic phenomena can be provided at the microscopic level by applying computer simulations.

5 Boltzmann–Matano method

Besides using an appropriate model of salt transport (necessarily coupled with moisture transport) with appropriate initial and boundary conditions, the accuracy of results depends critically on the precision with which one can determine the input transport and storage parameters in the model. The reason is that the input parameters may be strongly varying with the water content, salt concentration, or temperature. Varying input parameters are usually determined by inverse methods, and one such convenient inverse approach is the Boltzmann-Matano method [29, 30]. It is applicable for 1D transport and uses experimental data on the water content and salt concentration profiles.

When an inverse analysis is applied, the results are usually calculated numerically. Sometimes this approach may be quite laborious and not always reliable and, thus, verified by back-calculation of the original data. Moreover, the results are given just in a discrete format and may require final smoothing [31]. A great nuisance is also that the whole numerical procedure must be performed separately for each experiment. On the other hand, in an analytical approach these drawbacks are avoided and the results are obtained very fast. In such an approach the experimental data are approximated by analytical curves from which the resulting formulas are derived [32–34]. Here we shall illustrate such an analytical approach for the diffusion-advection model of Bear and Bachmat [35] that is able to describe a coupled water and salt transport.

This model takes into account salt dispersion in the liquid phase, the influence of moisture flow on salt transport, and the effect of bound salt on pore walls. It has been used to study, for instance, damage assessment of historical sandstone buildings and sculptures [36] and chloride transport in a lime plaster [8]. Analytical solutions to the model were obtained only in specific cases [37]. The input material parameters in the model are the moisture diffusivity κ in dependence on the volumetric moisture content w , salt diffusion coefficient D in dependence on the mass concentration C_f

of free salt in water, and the salt binding isotherm, i.e., the dependence of the concentration C_b of bound salt on the free salt concentration C_f . The measurable quantities are actually w , the total chloride concentration $C = wC_f + C_b$, and the binding isotherm $C_b = C_b(C_f)$. However, these three readily yield the free salt concentration C_f .

In the 1D case the model may be rewritten as [8]

$$\begin{aligned}\frac{\partial C}{\partial t} &= \frac{\partial}{\partial x} \left[wD(C_f) \frac{\partial C_f}{\partial x} + C_f \kappa(w) \frac{\partial w}{\partial x} \right], \\ \frac{\partial w}{\partial t} &= \frac{\partial}{\partial x} \left[\kappa(w) \frac{\partial w}{\partial x} \right].\end{aligned}\tag{5.1}$$

The initial and boundary conditions may be chosen as

$$\begin{aligned}C(0, t) &= C_0, & C(\infty, t) &= 0, & C(x, 0) &= 0, \\ w(0, t) &= w_0, & w(\infty, t) &= 0, & w(x, 0) &= 0,\end{aligned}\tag{5.2}$$

where C_0 and w_0 are positive constants, which corresponds to an initially dry sample.

The model can be subject to an inverse analysis, in particular to (an extension of) the Boltzmann-Matano method, using the Boltzmann variable $\eta = x/\sqrt{t}$. The final formulas read [8, 36]

$$\kappa(\eta) = \frac{I_1(\eta)}{2w'(\eta)}, \quad D(\eta) = -\frac{C_f(\eta) I_1(\eta)}{2w(\eta)C_f'(\eta)} + \frac{I_2(\eta)}{2w(\eta)C_f'(\eta)}\tag{5.3}$$

with

$$I_1(\eta) \equiv \int_{\eta}^{\infty} \eta^* w'(\eta^*) d\eta^*, \quad I_2(\eta) \equiv \int_{\eta}^{\infty} \eta^* C'(\eta^*) d\eta^*,\tag{5.4}$$

where the primes indicate derivatives with respect to η . When the moisture and total salt concentration profiles $w(x, t)$ and $C(x, t)$ are obtained from experiment, they may be easily expressed as η profiles $w(\eta)$, $C(\eta)$, and $C_f(\eta)$. Using these three profiles, one can calculate η dependences of the moisture diffusivity κ and salt diffusion coefficient D from Eq. (5.3). The plots of κ vs. w and of D vs. C_f follow from the plots of $\kappa(\eta)$ vs. $w(\eta)$ and $D(\eta)$ vs. $C_f(\eta)$ in which η varies over its whole range of values.

Rather than using numerical calculations, this procedure can work also when suitable analytical formulas are used to approximate the three input profiles. For S-shaped profiles the complementary error function, erfc , can be used,

$$w(\eta) \approx h_1 \operatorname{erfc} \left[\frac{\sqrt{\pi}}{2} a_1 (\eta - \eta_1) \right],\tag{5.5}$$

$$C(\eta) \approx h_2 \operatorname{erfc} \left[\frac{\sqrt{\pi}}{2} a_2 (\eta - \eta_2) \right], \quad (5.6)$$

and

$$C_f(\eta) \approx h_3 \operatorname{erfc} \left[\frac{\sqrt{\pi}}{2} a_3 (\eta - \eta_3) \right]. \quad (5.7)$$

The constants h_j , a_j , and η_j are fitting parameters obtained for a given set of experimental data. The error function was originally proposed by Hall [32]. The results for the plots of κ vs. w and of D vs. C_f can be obtained analytically as [32]

$$\kappa(w) \approx \frac{1}{\pi a_1^2} + \frac{\eta_1}{2a_1} y_w e^{E_w^2}, \quad (5.8)$$

where $E = \operatorname{erfc}^{-1}(w/h_1)$ is an inverse to the complementary error function, and [38]

$$D(C_f) \approx \frac{\frac{h_2}{a_2} \left(\frac{1}{\pi a_2} e^{-M_2^2} + \frac{\eta_2}{2} \operatorname{erfc} M_2 \right) - C_f \left(\frac{1}{\pi a_2} e^{-M_1^2} + \frac{\eta_1}{2} \operatorname{erfc} M_1 \right)}{a_3 h_3 \operatorname{erfc} M_1 e^{-F^2}}. \quad (5.9)$$

Here $F = \operatorname{erfc}^{-1}(C_f/h_3)$ and $M_i = (a_i/a_3)F + (\sqrt{\pi}/2)a_i(\eta_3 - \eta_i)$ with $i = 1, 2$.

Let us illustrate the method for an experiment in which a coupled moisture and chloride transport was studied in a sandstone. In the dry state the sandstone had the bulk density 1776 kg m^3 , matrix density 2531 kg m^3 , and total open porosity 0.297 . In the experiment dry prismatic samples of dimensions $20 \times 40 \times 160 \text{ mm}$ were exposed by their $20 \times 40 \text{ mm}$ face to a penetrating 1 M NaCl solution. The solution had the concentration $37 \text{ g of Cl}^-/\text{l}$ and the bulk density 1041 kg m^3 . The lateral sides of the samples were vapor-proof insulated to make the chloride solution transport practically one-dimensional. The moisture and chloride concentration profiles are shown in Fig. 5.1. The chloride binding isotherm $C_b = C_b(C_f)$ is almost linear for C_f up to 13 kg m^3 with a slope $K = 10.78$. The profile of the free chlorides is therefore given as $C_f(\eta) = C(\eta)/[w(\eta) + K]$ (see Fig. 5.1(c)).

The least-square fits of the erfc model profiles to the experimental ones are also plotted in Fig. 5.1. They are in reasonably good agreement with the data. The dependences of the moisture diffusivity on the moisture content and of the chloride diffusion coefficient on the free chloride concentration profile, as they follow from Eqs. (5.8) and (5.9) are plotted in Fig. 5.2. The dependence $D(C_f)$ diverges both at low and high concentrations. This is just a consequence of our choice of the model erfc profiles that tend to

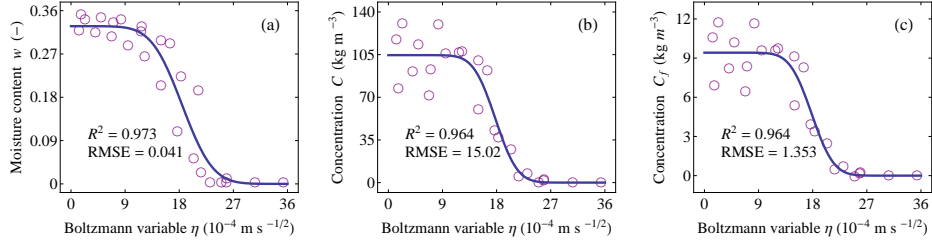


Figure 5.1: The profile of (a) the moisture content, (b) the total chloride concentration, and (c) obtained experimentally (circles) and their approximations by the erfc model profiles (curves).

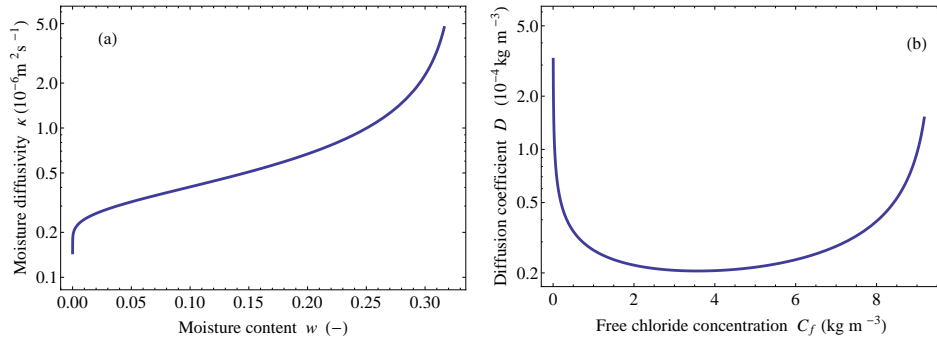


Figure 5.2: (a) The moisture dependence of the moisture diffusivity. (b) The concentration dependence of the chloride diffusion coefficient.

their maximal and minimal values at a Gaussian rate. At intermediate concentrations, however, various model profiles should yield practically the same results, provided they approximate the experimental data accurately. Therefore, for most concentrations D plotted in Fig. 5.2(b) is to be accurate, and the presented approach is a fast and reliable way for its estimation. Note that the values of D are three or four orders of magnitude higher than for free chloride ions in water, in agreement with other studies [8].

We carried out a comparison of several formulas for determining the concentration dependence of diffusion coefficients by the Boltzmann-Matano method in [39]. The formulas were expressed in terms of the Gauss error function, hyperbolic tangent, exponential, and inverse tangent, and the corresponding formulas for the diffusion coefficient were calculated. We demonstrated that even very similar profiles could lead to rather different diffusion coefficients, especially at low concentrations. Using two examples of different diffusion processes, we showed that the results can be employed to

rapidly calculate diffusion coefficients. In addition, it was shown that a finite diffusion coefficient at low concentrations only occurs if the corresponding concentration profile decays at a Gaussian rate or faster.

Bibliography

- [1] R. Černý and P. Rovnaníková. *Transport Processes in Concrete*. Spon Press, London, 2002.
- [2] J. R. Philip and D. A. De Vries. Moisture movement in porous materials under temperature gradients. *Trans. Amer. Geophys. Union*, 38:222, 1957.
- [3] T. Korecký, M. Keppert, J. Maděra, and R. Černý. Water transport parameters of autoclaved aerated concrete: Experimental assessment of different modeling approaches. *J. Build. Phys.*, 39:170–188, 2015.
- [4] S. R. de Groot and P. Mazur. *Non-Equilibrium Thermodynamics*. Dover Publications, New York, 1984.
- [5] M. Koniorczyk and D. Gawin. Heat and moisture transport in porous building materials containing salt. *J. Build. Phys.*, 31:279–300, 2008.
- [6] M. Koniorczyk and D. Gawin. Modelling of salt crystallization in building materials with microstructure - poromechanical approach. *Constr. Build. Mater.*, 36:860–873, 2012.
- [7] Z. Pavlík, M. Pavlíková, and R. Černý. Salt transport in water-saturated and dry specimens of building materials. In *1st Central European Symposium on Building Physics*, pages 157–162, Technical University of Lodz, 2010.
- [8] Z. Pavlík, L. Fiala, J. Maděra, M. Pavlíková, and R. Černý. Computational modelling of coupled water and salt transport in porous materials using diffusion-advection model. *J. Frankl. Inst.*, 348:1574, 2011.
- [9] R. Valiullin, P. Kortunov, J. Kärger, and V. Timoshenko. Surface self-diffusion of organic molecules adsorbed in porous silicon. *J. Phys. Chem. B*, 109:5746–5752, 2005.

- [10] M. Dvoyashkin, A. Khokhlov, S. Naumov, and R. Valiullin. Pulsed field gradient nmr study of surface diffusion in mesoporous adsorbents. *Micropor. Mesopor. Mater.*, 125:58–62, 2009.
- [11] K. Miyabe and G. Guiochon. Fundamental interpretation of the peak profiles in linear reversed-phase liquid chromatography. *Adv. Chromatogr.*, 40:1–113, 2000.
- [12] K. Miyabe and G. Guiochon. Measurement of the parameters of the mass transfer kinetics in high performance liquid chromatography. *J. Sep. Sci.*, 26:155–173, 2003.
- [13] A. Kapoor, R. T. Yang, and C. Wong. Surface diffusion. *Catal. Rev.–Sci. Eng.*, 31:129–214, 1989.
- [14] H. D. Do, D. D. Do, and I. Prasetyo. On the surface diffusion of hydrocarbons in microporous activated carbon. *Chem. Eng. Sci.*, 56:4351–4368, 2001.
- [15] **I. Medved’** and R. Černý. Surface diffusion in porous media: A critical review. *Micropor. Mesopor. Mat.*, 142:405–422, 2011.
- [16] H. L. Frisch. The time lag in diffusion. *J. Phys. Chem.*, 61:93–95, 1957.
- [17] D. D. Do and H. D. Do. Analysis of dual diffusion and non-linear adsorption isotherm with a time lag method. *Adsorption*, 6:111–123, 2000.
- [18] T. Alla-Nissila, R. Ferrando, and S. C. Ying. Collective and single particle diffusion on surfaces. *Adv. Phys.*, 51:949–1078, 2002.
- [19] J. V. Barth. Transport of adsorbates at metal surfaces: from thermal migration to hot precursors. *Surf. Sci. Rep.*, 40:75–149, 2000.
- [20] C. Borgs and R. Kotecký. A rigorous theory of finite-size scaling at first-order phase transitions. *J. Stat. Phys.*, 61:79–119, 1990.
- [21] **I. Medved’** and A. Trník. Many-particle surface diffusion coefficients near first-order phase transitions at low temperatures. *Phys. Rev. E*, 86:011601, 2012.
- [22] **I. Medved’** and A. Trník. Collective surface diffusion near a first-order phase transition. *Phys. Rev. B*, 83:233406, 2011.

- [23] **I. Medved'** and A. Trník. Surface diffusion near first-order phase transitions for a model of on a triangular lattice. *J. Stat. Mech.*, page P01025, 2012.
- [24] **I. Medved'** and A. Trník. Multi-site correlation functions in surface diffusion. *J. Stat. Mech.*, page P04026, 2013.
- [25] **I. Medved'**, J. Avsec, J. Kováč, and A. Trník. Rigorous results on surface diffusion coefficients near a first-order phase transition. *Int. J. Thermophys.*, 35:1853–1862, 2014.
- [26] **I. Medved'** and R. Černý. Osmosis in porous media: A review of recent studies. *Micropor. Mesopor. Mat.*, 170:299–317, 2013.
- [27] J. D. Sherwood and B. Craster. Transport of water and ions through a clay membrane. *J. Colloid Interf. Sci.*, 230:349–358, 2000.
- [28] S. Bader and H. Kooi. *Adv. Water Res.*, 28:203–214, 2005.
- [29] L. Boltzmann. Zur integration des diffusionsgleichung bei variabeln diffusions coefficienten. *Wiedemanns Ann. Phys.*, 53:959, 1894.
- [30] C. Matano. On the relation between the diffusion-coefficients and concentrations of solid metals (the nickel-copper system). *Jpn. J. Phys.*, 8:109, 1933.
- [31] J. Carmeliet, H. Hens, S. Roels and O. Adan, H. Brocken, R. Cerny, Z. Pavlik, C. Hall, K. Kumaran, and L. Pel. Determination of the liquid water diffusivity from transient moisture transfer experiments. *J. Therm. Env. Bldg. Sci.*, 27:277, 2004.
- [32] L. D. Hall. An analytical method of calculating variable diffusion coefficients. *J. Chem. Phys.*, 21:87, 1953.
- [33] S. K. Kailasam, J. C. Lacombe, and M. E. Glicksman. Evaluation of the methods for calculating the concentration-dependent diffusivity in binary systems. *Metall. Mater. Trans. A*, 30:2605, 1998.
- [34] M. Vach and M. Svojtka. Evaluation of molar volume effect for calculation of diffusion in binary systems. *Metall. Mater. Trans. B*, 43:1446, 2012.
- [35] J. Bear and Y. Bachmat. *Introduction to Modelling of Transport Phenomena in Porous Media*, volume 4. Kluwer, Dordrecht, 1990.

- [36] Z. Pavlík, P. Michálek, M. Pavlíková, I. Kopecká, I. Maxová, and R. Černý. Water and salt transport and storage properties of mšené sandstone. *Constr. Build. Mater.*, 22:1736, 2008.
- [37] A. Kumar, D. K. Jaiswal, and N. Kumar. Analytical solutions of one-dimensional advectiondiffusion equation with variable coefficients in a finite domain. *J. Earth Syst. Sci.*, 118:539, 2009.
- [38] **I. Medved'** and R. Černý. Coupled water and salt transport in porous materials: Rapid determination of a varying diffusion coefficient from experimental data. *Transp. Porous Med.*, 105:597–610, 2014.
- [39] **I. Medved'** and R. Černý. Model formulas for facilitating determination of concentration-dependent diffusion coefficients. *Met. Mater. Int.*, 21:907–912, 2015.

Curriculum Vitae — Igor Medved’

Date and place of birth: June 28, 1973, Levice, Slovakia

Higher education

PhD 2001, Charles University, Prague (theoretical physics)

MSc 1996, Charles University, Prague (theoretical physics)

Professional appointments

Since 2014: Associate Professor — Czech Technical University, Prague

2010 – 2014: Research Fellow — Czech Technical University, Prague

Since 2004: Associate Professor — Constantine the Philosopher University
Nitra, Slovakia

2003: Research Fellow — Institute of Electrical Engineering
Slovak Academy of Sciences, Bratislava

2001 – 2002: Research Fellow — Texas Christian University, Fort Worth, TX, USA

2000: Research Fellow — University of Groningen, Groningen, the Netherlands

1999 – 2000: Research Fellow — Nuclear Physics Institute
Czech Academy of Sciences, Řež

Professional experience

Principal investigator of 1 international and 2 national scientific projects, team member of 3 European and 11 national scientific projects. Member of the permanent International Organizing Committee of the European Conferences on Thermophysical Properties, co-chair of the international conference Thermophysics 2015, and member of the scientific committee of Thermophysics 2010, 2011, and 2012. Robert A. Welch Foundation Postdoctoral Fellow (2001–2002, 2004, 2006, 2007). Reviewer to the International Journal of Thermophysics, Heat and Mass Transfer, Journal of Chemical Physics, and Metallic Materials.

Scientific publications

Author and co-author of 39 WoS papers, 66 SCI citations, 12 papers in reviewed international journals, h-index 6.

Teaching

Advisor to 6 Bc, 8 MSc, and 3 PhD theses. Author of 1 textbook and 3 teaching texts.